Title

Matrix stiffness modulates the differentiation of neural crest stem cells in vivo

Journal

Journal of Cellular Physiology, 234(5)

ISSN

0021-9541

Authors

Zhu, Yiqian
Li, Xian
Janairo, Randall Raphael R
et al.

Publication Date

2019-05-01

DOI

10.1002/jcp.27518

Peer reviewed

Published in final edited form as:

J Cell Physiol. 2019 May ; 234(5): 7569–7578. doi:10.1002/jcp.27518.

Matrix Stiffness Modulates the Differentiation of Neural Crest Stem Cells *In Vivo*

Yiqian Zhu[1,2], **Xian Li**[1,3], **Randall Raphael R. Janairo**[1], **George Kwong**[1], **Anchi D. Tsou**[1], **Julia S. Chu**[1], **Aijun Wang**[4], **Jian Yu**[1,2], **Dong Wang**[5], **Song Li**[1,5,6,*]

[1]Department of Bioengineering, University of California, Berkeley, CA 94720, USA

[2]Department of Neurosurgery, Fudan University Huashan Hospital, Shanghai 200040, China

[3]Laboratory of Biomedical Engineering, Chongqing Medical University, Chongqing 400016, China

[4]Department of Surgery, School of Medicine, University of California, Davis, Sacramento, CA 95817, USA

[5]Department of Bioengineering, University of California, Los Angeles, CA 90095, USA

[6]Department of Medicine, University of California, Los Angeles, CA 90095, USA

Abstract

Stem cells are often transplanted with scaffolds for tissue regeneration; however, how the mechanical property of a scaffold modulates stem cell fate *in vivo* is not well understood. Here we investigated how matrix stiffness modulates stem cell differentiation in a model of vascular graft transplantation. Multipotent neural crest stem cells (NCSCs) were differentiated from induced pluripotent stem cells, embedded in the hydrogel on the outer surface of nanofibrous polymer grafts, and implanted into rat carotid arteries by anastomosis. After 3 months, NCSCs differentiated into smooth muscle cells (SMCs) near the outer surface of the polymer grafts; in contrast, NCSCs differentiated into glial cells in most part of the hydrogel. Atomic force microscopy demonstrated a stiffer matrix near the polymer surface but much lower stiffness away from the polymer graft. Consistently, *in vitro* studies confirmed that stiff surface induced SMC genes while soft surface induced glial genes. These results suggest that the scaffold's mechanical properties play an important role in directing stem cell differentiation *in vivo*, which has important implications in biomaterials design for stem cell delivery and tissue engineering.

Keywords

Neural crest stem cells; Matrix stiffness; Vascular tissue engineering; Nanofibrous scaffold; Smooth muscle cells; Glial cells

[*]Corresponding address: Song Li, Ph.D., Department of Bioengineering and Department of Medicine, University of California, Los Angeles, 5121 Engineering V, Los Angeles, CA 90095, songli@ucla.edu.

Disclosure

The authors declare no competing financial interests.

1. Introduction

Stem cells have tremendous potential for regenerative medicine applications. Stem cells can be either seeded into scaffolds to engineer functional tissues such as blood vessels[1], or injected into tissues within delivery matrix to retain cells locally and enhance cell survival[2–4]. Besides the biochemical properties, the biophysical properties such as the stiffness and micro/nano topography also play important roles in regulating cell functions and tissue remodeling[5–12]. Although these effects have been widely studied *in vitro*, their *in vivo* effects on cell differentiation and tissue remodeling are not well understood. Here we used induced pluripotent stem cells (iPSCs)-derived multipotent neural crest stem cells (NCSCs) to investigate how matrix stiffness regulated stem cell differentiation in a vascular graft implantation model.

iPSC provides an unlimited cell source for the derivation of various cell types for the applications such as regenerative medicine and disease modeling[13–16]. iPSCs are capable of differentiating into various cell types such as neural lineages (peripheral neurons and Schwann cells)[17], mesenchymal lineages (smooth muscles, osteoblasts, chondrocytes, and adipocytes)[15], hematopoietic precursors[18] and hepatocytes[19]. NCSCs are multipotent, and can differentiate into both mesenchymal and neural lineages[20,21], which represents a useful model to study multipotent stem cell differentiation *in vivo*. Our previous study has shown that human iPSC-derived NCSCs can be seeded into nerve conduits to enhance peripheral nerve regeneration[22]. In this case, NCSCs differentiate into Schwann cells to facilitate the myelination of regenerated axons, suggesting stem cell differentiation *in vivo* is context dependent and regulated by local tissue environment. On the other hand, NCSCs can differentiate into vascular smooth muscle cells (SMCs) or perivascular cells[23], and can be used to regenerate blood vessels. However, it is not known how the vascular niche regulates NCSC differentiation *in vivo*.

We and others have used electrospinning technology to fabricate tissue-engineered vascular grafts (TEVGs)[1,24]. Electrospun nanofibers of polymers coated with matrix proteins allow the adhesion, proliferation and organized assembly of cells *in vitro*[25–27], and the structure of electrospun scaffolds can help create a microenvironment of extracellular matrix (ECM) for the cells. For example, aligned nanofibers facilitated cell organization, infiltration and matrix remodeling[1,28]. Thus, the nanofibrous scaffold with fiber alignment could be considered as a model to investigate the remodeling of vascular graft *in vivo*. Based on the structure of native blood vessel, a one-step procedure was developed in this study to fabricate vascular grafts with a bi-layer structure similar to native artery: the luminal surface has longitudinally aligned nanofibers for EC migration, and the outer layer has circumferentially aligned nanofibers for SMC organization and structural support. Here we used this bi-layer scaffold seeded with NCSCs as a model to investigate the differentiation of iPSC-derived NCSCs regulated by matrix stiffness in the vascular niche.

2. Materials and Methods

The commercial sources of reagents are listed in Supplemental Table 1.

2.1. Cell Culture, NCSC Derivation and Differentiation

Human iPSCs derived from fibroblasts were obtained from Dr. George Daley's laboratory. The derivation of NCSCs was described in detail previously[22]. Briefly, iPSCs were made into embryonic bodies to form rosettes, which were mechanically harvested, cultured in suspension, and transferred to monolayer culture. NCSCs were derived by clonal expansion and p75+/HNK1+ clones were further expanded and used for experiments. NCSCs derived from iPSCs were maintained in StemPro® NSC serum-free neural induction medium (SFM) without differentiation. To test the multipotency of NCSCs, cell differentiation into mesenchymal and neural lineages was carried out using the protocol described previously[20,29,30].

For all experiments, NCSCs (Passages 4–8) with 70–80% confluency were used. Unless specified, experiments in vitro were performed in the cell culture medium of DMEM supplemented with 10% FBS and 1% penicillin/streptomycin.

2.2. Biochemical Analysis

Immunostaining, microscopy and quantitative polymerase chain reaction (qPCR) analysis were performed as described previously[30]. The primer sequences for the genes of interest are listed in Supplemental Table 2. The level of gene expression was normalized to the amount of 18S ribosomal RNA in the same sample.

2.3. Fabrication of Substrates with Different Stiffness

The first method involved the control of matrigel thickness. Matrigel was prepared by mixing a cold matrigel stock solution and DMEM medium at 2:1 ratio (volume to volume). The soft substrate was matrigel with about 500μm thickness. For stiff substrates, matrigel solution (before polymerization) was used to rinse the culture dishes, and excess solution was removed, resulting in a thin layer (microns) coating of polymerized matrigel.

The second method was to make polyacrylamide (PA) gels with different amount of crosslinker as described previously[5,31]. Briefly, glass slides were treated with 3-aminopropyltrimethoxysilane and 0.5% glutaraldehyde. PA gel solution with 6% acrylamide and different bis-acrylamide concentrations (0.5%, 0.05%) was allowed to polymerize to form 200-μm thick gel on the slides. Sulfo-SANPAH was used to link collagen-I (10 μg/cm^2) to the PA gel surface. Stiff substrates (glass slides) were coated with the same density of collagen-I. All substrates were sterilized by UV. A Comparator was used to measure the stiffness of PA gels in response to a known force[5].

2.4. Bi-layer Vascular Scaffold Fabrication and Characterization

Poly(L-lactide) (PLLA) (1.09 dL/g inherent viscosity; Lactel Absorbable Polymers) was dissolved in 1,1,1,3,3-hexafluoro-2-propanol (HFIP) by means of sonication for 30 min or until all of the PLLA crystals were completely dissolved, resulting in 19% (w/v) solution. Nonwoven aligned nanofibrous vascular scaffolds composed of PLLA were fabricated using a customized electrospinning process. The tubular scaffold comprised a luminal region of longitudinally aligned nanofibers and an outer region of circumferentially oriented nanofibers. PLLA were dissolved in a volatile organic solvent, hexafluoroisopropanol

(HFIP). The electrospinning apparatus consisted of a syringe pump capable of delivering the polymer solution to the tip of a needle secured onto a mechanized platform suspended over a 1-mm outer diameter rotating mandrel collector assembly. The needle platform was charged by a positive-polarity power supply and the mandrel assembly was charged by a negative-polarity power supply. To make the inner layer with longitudinally aligned nanofibers, the jet stream of PLLA (19% weight/volume) solution from the spinneret whipped between the two conductive ends of a plastic mandrel, resulting aligned nanofibers on the non-conductive portion in the middle of a slowly rotating mandrel. The outer layer with circumferentially oriented nanofibers was generated using a high-speed rotating mandrel at 800 rpm, instead of a low-speed rotation to produce randomly oriented nanofibers.

Upon completion of electrospinning, the vascular scaffolds were air-dried on the mandrel collector for two nights to remove residual HFIP. The scaffolds were then rinsed in the deionized water and cut to an appropriate length. All scaffolds were sterilized with ethylene oxide gas before characterization and *in vivo* implantation studies. The alignment of nanofibers and the structure of the nanofibrous vascular scaffolds were examined by scanning electron microscopy (SEM). The diameter of nanofibers ranged from 500–800 nm.

2.5. Cell Seeding on Polymer Scaffold and Characterization

The nanofibrous scaffolds were sterilized by ethylene oxide gas sterilization before use. NCSCs were detached by trypsin and re-suspended in the SFM (2×10^4 cells/μl). The cell suspension was mixed with a cold matrigel solution at 2:1 ratio (volume to volume), and then injected into the space around the tubular scaffold in a casting tube (*e.g.* 1ml for one scaffold 1.2 cm in length). The scaffolds were kept in the incubator at 37 °C for more than an hour, and NCSC maintenance medium was added to cover the scaffolds. The culture was maintained in the incubator overnight before surgery. Live/dead assay was used to assess the viability of NCSCs in the matrigel-cellular nanofibrous vascular scaffolds.

2.6. *In vivo* Implantation

All animal procedures were approved by the Institutional Animal Care and Use Committee (IACUC) at UC Berkeley and were carried out according to the institutional guidelines and National Institutes of Health Guide for Care and Use of Laboratory Animals. Adult athymic rats (National Cancer Institute) weighing 200±20 g were anesthetized with 1.5% isoflurane in 70% N_2O/30% O_2. Toe pinch was used to confirm the anesthetic depth. Body temperature was maintained at 37.0±0.5°C during surgery. Briefly, the rat was set in a supine position, and a midline incision was made on the ventral side of the neck to expose the left common carotid artery (CCA). Under a surgical microscope, the carotid artery was isolated and the segment of the artery was clamped temporarily. Matrigel-cellular scaffold was used to place end-to-end to the CCA and sutured with 10–0 interrupted stitches. The muscle layers were approximated with interrupted 4–0 nylon sutures and stainless steel wound clips were used to close the skin wound. Buprenorphine was given to the animals for analgesia. Retrieval of the graft involved the same initial steps for implantation. The graft was removed by ligation of native CCA directly adjacent to the suture locations.

2.7. Histological Analysis

The vascular grafts were explanted and fixed in 4% paraformaldehyde at 4°C. Cross sections in the middle portion of the graft (10 μm in thickness; 5–7 mm from the proximal end of the graft) were cryosectioned for H&E staining and immunostaining. The frozen sections (10 μm in thickness) of vascular grafts were incubated in 5% normal goat serum for 30 minutes to block the non-specific binding, and then incubated with primary antibody diluted in 5% normal goat serum overnight at 4°C. Negative controls were included by omitting the primary antibody. The sections were incubated for one hour with either horseradish peroxidase-conjugated anti-mouse or rabbit IgG (1:1000, Alexa 594 for red and Alexa 488 for green, Invitrogen, Carlsbad, CA). Finally, slides were mounted and examined by using a fluorescence microscope (Zeiss Axioskop 2 MOT). For immunohistochemical staining, the sections were incubated with biotin-conjugated secondary antibody and avidin-biotin enzyme reagent for 1 h. A hematoxylin and eosin (H&E) counterstaining was performed. For H&E staining, sections were deparaffinized first in three changes of 100% xylene for 5 minutes each, then hydrated through graded alcohol (100%, 95% and 70%; 5 min each), and rinsed in phosphate-buffered saline, followed by standard H&E staining.

2.8. Atomic Force Microscopy (AFM) Measurement of Matrix Stiffness

Animals were sacrificed following three months of vascular graft implantation. Vascular graft samples were removed from the animal and cryopreserved using OCT compound. Samples were frozen for at least 24 hours prior to cryosectioning. Samples were then sectioned into 90 μm slices, mounted onto microscope slides, and allowed to dry for one hour. Sections were rehydrated using PBS and washed three times to dissolve the OCT compound. Samples remained hydrated throughout AFM testing. Force displacement profiles were created using silicon nitride cantilevers with pyramidal tips in contact mode. Cantilever spring constants were measured using thermal calibration in order to avoid error due to manufacturing discrepancies. Each tissue area was probed ten times to avoid inconsistencies due to tissue heterogeneity. A customized MATLAB program was then used to apply the Hertz model to the data and determine the elastic modulus of the samples.

2.9. Statistical Analysis

Mean and standard deviation (SD) values were calculated for each group of data. Analysis of variance (ANOVA) was performed to detect whether a significant difference ($p<0.05$, $n\geq3$) existed between groups. The Holm *t-test* was used to identify any differences. Student's *t-test* was used to analyze experimental groups with two samples. For the data with the normalization to the respective controls, log-transformed *t-test* was used to determine whether there was significant difference.

3. Results

3.1. NCSC Characterization

NCSCs were derived from iPSCs, clonal expanded, and characterized by the expression of markers P75, HNK1, vimentin and nestin (Figure 1 A–D)[22]. NCSCs were capable of differentiating into neural lineages, including glial cells (Figure 1 E–F) and peripheral

neurons (Figure 1 G–H). In addition, NCSCs could differentiate into mesenchymal lineages such as SMCs (Figure 1 I–J), adipogenic cells (Figure 1 K–L), osteogenic cells (Figure 1 M–N) and chondrogenic cells (Figure 1 O–P).

3.2. Cell-Seeded Nanofibrous Vascular Scaffold

Electrospun nanofibrous vascular scaffold with an inner diameter (ID) of 1mm and the thickness of 100 μm were produced (Figure 2A). SEM images showed longitudinally aligned nanofibers (Figure 2B) in the luminal layer (~30 μm in thickness), which provided the guidance for the growth and migration of ECs and facilitate cell infiltration into the three-dimensional (3D) scaffold. Meanwhile, the outer layers (~70 μm in thickness) with circumferentially aligned nanofibers (Figure 2C) were generated outside of the longitudinally aligned nanofibers, which enhanced ECM remodeling and mechanical property of the scaffolds.

NCSCs were mixed with matrigel and seeded around the nanofibrous vascular graft. One day later, cell contraction resulted in the compaction of the gel around the grafts (Figure 2D), and live/dead assays showed >95% cells were calcein positive (live/green) and ethidium bromide negative (dead/red) (Figure 2E), indicating that the seeded cells were viable.

Cell-seeded nanofibrous vascular grafts were implanted into rat carotid artery by anastomosis. At 3 months post surgery, the grafts showed integration with the host artery (Figure 2F). CD31 staining showed endothelial cell (EC) coverage on the luminal surface, which was important to maintain the long-term patency of grafts, and there was also some EC infiltration in the outer layer (Figure 2G), likely migrating from the surrounding microvessels.

3.3. Differentiation of NCSCs in the vascular grafts *in vivo*

To assess NCSC differentiation in vascular grafts, the cross sections of the explants were double-stained for human antigen NuMA and differentiation markers ACTA2, MHC and GFAP (Figure 3). $ACTA2^+$, MHC^+ and $GFAP^+$ stainings were negative in the implanted NCSCs at 2-week time point (data not shown). At 3 months, $NuMA^+/ACTA2^+$ and $NuMA^+/MHC^+$ cells were found on the outer surface of the polymer scaffold, i.e., the boundary of the polymer scaffold and the fibrous capsule layer derived from the matrigel layer (Figure 3 A–H). Interestingly, $NuMA^+$ cells in the matrigel layer further away from the boundary were negative for ACTA2 and MHC. Instead, these $NuMA^+$ cells were $GFAP^+$ (Figure 3 I–L), suggesting that the implanted NCSCs might differentiate into glial cells in the outer matrigel layer.

3.4. AFM Measurement of Matrix Stiffness around the Polymer Grafts

Since transplanted NCSCs in matrigel experienced similar biochemical factors in the vascular niche, we postulated that the mechanical property of matrix could modulate NCSC differentiation. To test this possibility, we utilized AFM to measure the mechanical property of the regions where we found differential SMC (region I) and glial (region II) marker expression (Figure 4A). AFM measurement of elastic modulus (Figure 4 B) showed that the

polymer scaffold and the native carotid artery had similar stiffness (~ 6000 kPa) (Figure 4 B); Interestingly, the fibrous capsule layer around the graft scaffold had a gradient pattern of stiffness with stiffer matrix in the inner layer (region I, ~50 kPa) and softer in the outer layer (region II, ~10 kPa) (Figure 4 B).

3.5. Effect of Matrigel-Coated Soft and Stiff Surfaces on NCSC Differentiation *In Vitro*

To directly determine the effects of substrate stiffness on NCSC differentiation, we cultured NCSCs on matrigel solution-coated culture wells (~ 1 GPa) or thick matrigel (< 1 kPa) in DMEM medium supplemented with 10% FBS, to mimic the two extreme ends of the stiffness gradient of the graft microenvironment *in vivo*. Interestingly, the expression of SMC markers ACTA2 and CNN1 were shown on matrigel-coated stiff substrates, but undetectable on soft matrigel after 1 week of culture (Figure 5 A–D). In contrast, glial marker GFAP expressed strongly on soft matrigel but not on matrigel-coated stiff substrates (Figure 5 E–F). In addition, qPCR analysis (Figure 5G) showed the same trend as the immunostaining results, suggesting substrate stiffness may regulate NCSC differentiation.

3.6. Effects of Substrate Stiffness on NCSC Differentiation *In Vitro*

Since matrigel-coated surfaces only allowed the comparison of very soft (< 1 KPa) and very stiff (~ 1 GPa) surfaces, we used polyacrylamide (PA) gel to make surfaces with well-defined stiffness in the range of KPa. In addition, we used collagen-I as the coating matrix protein to avoid the undefined matrigel components and to determine whether the stiffness effect was matrix protein dependent.

Phalloidin staining of actin cytoskeleton (Figure 6 A–C) and Vinculin staining of cell adhesion (Figure 6 D–F) demonstrated that NCSCs on stiff substrates (1 GPa, Figure 6 A and D) had extensive stress fibers and large focal adhesions. Cells on lower stiffness (15kPa and 1kPa, Figure 6 B–C and E–F) had monotonic decrease in spreading area, focal adhesions and stress fibers.

Gene analysis demonstrated that NCSCs on stiff substrates (1 GPa) had much higher expression levels of SMC markers ACTA2 than cells on PA gels (15 kPa and 1 kPa). CNN1 expression showed a monotonic decrease with the stiffness. In contrast, the decrease in stiffness induced a monotonic increase of glial marker GFAP (Figure 6 G). These results strongly suggested that matrix stiffness modulated NCSC differentiation into smooth muscle and neural lineages in a stiffness-dependent manner: high stiffness induced the expression of SMC markers, while low stiffness induced the expression of glial markers.

4. Discussion

Stem cell transplantation is a promising approach for tissue regeneration. To guide stem cell differentiation to the desired cell types *in vivo*, both biochemical and biophysical factors are important. A major finding in this study is that matrix stiffness is critical for stem cell differentiation *in vivo*. In the vascular niche, many other microenvironmental cues are present, including the cyclic mechanical stretch in the vascular wall and various growth factors. Nevertheless, these microenvironmental factors are not sufficient to direct NCSC differentiation into SMCs. The differentiation of NCSCs into SMCs only happened near the

stiff surface (50 kPa or higher) of the polymer scaffold. In the outer soft area (< 15 kPa), some NCSCs differentiate into glial cells. *In vitro* experiments also confirmed this critical role of stiffness in NCSC differentiation. Thus, when stem cells are seeded onto scaffolds or encapsulated for injection, the mechanical property of the scaffolds/matrix can be engineered to enhance the desired therapeutic effect. Another interesting finding is that the cells cultured on matrigel or collagen-I-coated surfaces showed similar responses to the stiffness of the substrates. This result further underlines the importance of matrix stiffness on the differentiation of stem cells.

The electrospun polymer scaffold has a stiffness similar to native artery, and this mechanical compliance matching makes the electrospun polymer scaffold appropriate for vascular graft fabrication. In addition, the biomimetic micro/nano structure of the scaffold, although it is not the focus of this study, may have advantage for vascular remodeling. The longitudinally aligned fibers on the inner surface may facilitate EC migration and endothelialization to maintain the patency of the vascular grafts, while the circumferential aligned fibers on the outer layer may facilitate the organization of SMCs and ECM remodeling to improve the mechanical property. It appears that there is tissue ingrowth into the loosely organized fibers on the outer surface, but the porosity of the electrospun scaffold needs to be increased to further promote cell infiltration throughout the wall thickness.

The *in vitro* studies using both matrigel and PA gel coated with collagen-I show that NCSC differentiation is regulated by substrate stiffness, which provides a mechanistic explanation of the observation *in vivo*. The stiffness regulation of stem cell differentiation *in vivo* is not limited to the vascular niche. For example, when NCSCs are encapsulated in matrigel and transplanted into nerve conduits, NCSCs in the middle of the conduits differentiate into Schwann cells to facilitate axon growth and myelination[22], which suggests that the differentiation of stem cells is indeed regulated by the microenvironment of the nervous tissue. However, we did observe that NCSCs on the inner surface of the nerve conduits differentiated into myofibroblast-like cells (data not shown), suggesting the stiffness of the scaffold also plays an important role in cell fate determination.

It should be noted that *in vivo* microenvironment is complex, which includes a variety of biophysical and biochemical factors such as growth factors and matrix proteins. Further investigation is needed to understand the effects of all these individual factors and their combinations on stem cell fate decision. Altogether, these results provide insight into the interconnections between biophysical and biochemical signals in regulating stem cell differentiation, which will have significant impact on scaffold engineering and stem cell transplantation for regenerative medicine applications.

5. Conclusion

The differentiation of transplanted stem cells *in vivo* is not only regulated by biochemical factors, but also modulated by the stiffness of ECM. In this vascular graft-NCSC transplantation model, NCSCs differentiated into SMCs in the stiff matrix, and became glial cells in the soft matrix. This study provides a rational basis for the design of mechanically compatible biomaterials for stem cell therapies and tissue regeneration.

Supplementary Material

Refer to Web version on PubMed Central for supplementary material.

Acknowledgement

This project was supported in part by grants from National Institute of Health (EB012240, HL083900, HL117213 and HL121450), Telemedicine and Advanced Technology Research Center (TATRC), The Science and Technology Commission of Shanghai Municipality Project (13PJ1401300) and Shanghai Municipal Commission of health and Family Planning Project (201640306).

References

1. Hashi CK et al. Antithrombogenic property of bone marrow mesenchymal stem cells in nanofibrous vascular grafts. Proc Natl Acad Sci U S A 104, 11915–11920, doi:10.1073/pnas.0704581104 (2007). [PubMed: 17615237]
2. Levenberg S et al. Differentiation of human embryonic stem cells on three-dimensional polymer scaffolds. Proc Natl Acad Sci U S A 100, 12741–12746, doi:10.1073/pnas.1735463100 (2003). [PubMed: 14561891]
3. Huang NF, Yu J, Sievers R, Li S & Lee RJ Injectable biopolymers enhance angiogenesis after myocardial infarction. Tissue Eng 11, 1860–1866, doi:10.1089/ten.2005.11.1860 (2005). [PubMed: 16411832]
4. Mooney DJ & Vandenburgh H Cell delivery mechanisms for tissue repair. Cell stem cell 2, 205–213, doi:10.1016/j.stem.2008.02.005 (2008). [PubMed: 18371446]
5. Park JS et al. The effect of matrix stiffness on the differentiation of mesenchymal stem cells in response to TGF-beta. Biomaterials 32, 3921–3930, doi:10.1016/j.biomaterials.2011.02.019 (2011). [PubMed: 21397942]
6. Huang NF et al. Myotube assembly on nanofibrous and micropatterned polymers. Nano letters 6, 537–542, doi:10.1021/nl060060o (2006). [PubMed: 16522058]
7. Discher DE, Janmey P & Wang YL Tissue cells feel and respond to the stiffness of their substrate. Science 310, 1139–1143, doi:10.1126/science.1116995 (2005). [PubMed: 16293750]
8. Discher DE, Mooney DJ & Zandstra PW Growth factors, matrices, and forces combine and control stem cells. Science 324, 1673–1677, doi:10.1126/science.1171643 (2009). [PubMed: 19556500]
9. Peyton SR, Kim PD, Ghajar CM, Seliktar D & Putnam AJ The effects of matrix stiffness and RhoA on the phenotypic plasticity of smooth muscle cells in a 3-D biosynthetic hydrogel system. Biomaterials 29, 2597–2607, doi:10.1016/j.biomaterials.2008.02.005 (2008). [PubMed: 18342366]
10. Murphy KC et al. Hydrogel biophysical properties instruct coculture-mediated osteogenic potential. The FASEB Journal 30, 477–486, doi:10.1096/fj.15-279984 (2016). [PubMed: 26443826]
11. Luna JI et al. Multiscale Biomimetic Topography for the Alignment of Neonatal and Embryonic Stem Cell-Derived Heart Cells. Tissue Engineering Part C: Methods 17, 579–588, doi:10.1089/ten.tec.2010.0410 (2011). [PubMed: 21235325]
12. Wang D et al. Tissue-specific mechanical and geometrical control of cell viability and actin cytoskeleton alignment. Scientific reports 4, 6160, doi:10.1038/srep06160 (2014). [PubMed: 25146956]
13. Park IH et al. Disease-specific induced pluripotent stem cells. Cell 134, 877–886, doi:10.1016/j.cell.2008.07.041 (2008). [PubMed: 18691744]
14. Ebert AD et al. Induced pluripotent stem cells from a spinal muscular atrophy patient. Nature 457, 277–280, doi:10.1038/nature07677 (2009). [PubMed: 19098894]
15. Lian Q et al. Functional mesenchymal stem cells derived from human induced pluripotent stem cells attenuate limb ischemia in mice. Circulation 121, 1113–1123, doi:10.1161/CIRCULATIONAHA.109.898312 (2010). [PubMed: 20176987]

16. Hirschi KK, Li S & Roy K Induced pluripotent stem cells for regenerative medicine. Annu Rev Biomed Eng 16, 277–294, doi:10.1146/annurev-bioeng-071813-105108 (2014). [PubMed: 24905879]
17. Hu BY et al. Neural differentiation of human induced pluripotent stem cells follows developmental principles but with variable potency. Proc Natl Acad Sci U S A 107, 4335–4340, doi:10.1073/pnas.0910012107 (2010). [PubMed: 20160098]
18. Grigoriadis AE et al. Directed differentiation of hematopoietic precursors and functional osteoclasts from human ES and iPS cells. Blood 115, 2769–2776, doi:10.1182/blood-2009-07-234690 (2010). [PubMed: 20065292]
19. Song Z et al. Efficient generation of hepatocyte-like cells from human induced pluripotent stem cells. Cell Res 19, 1233–1242, doi:10.1038/cr.2009.107 (2009). [PubMed: 19736565]
20. Lee G et al. Isolation and directed differentiation of neural crest stem cells derived from human embryonic stem cells. Nat Biotechnol 25, 1468–1475, doi:10.1038/nbt1365 (2007). [PubMed: 18037878]
21. Sieber-Blum M & Hu Y Epidermal neural crest stem cells (EPI-NCSC) and pluripotency. Stem cell reviews 4, 256–260, doi:10.1007/s12015-008-9042-0 (2008). [PubMed: 18712509]
22. Wang A et al. Induced pluripotent stem cells for neural tissue engineering. Biomaterials 32, 5023–5032, doi:10.1016/j.biomaterials.2011.03.070 (2011). [PubMed: 21514663]
23. Wang A et al. Derivation of smooth muscle cells with neural crest origin from human induced pluripotent stem cells. Cells, tissues, organs 195, 5–14, doi:10.1159/000331412 (2012). [PubMed: 22005509]
24. Yu J et al. The effect of stromal cell-derived factor-1alpha/heparin coating of biodegradable vascular grafts on the recruitment of both endothelial and smooth muscle progenitor cells for accelerated regeneration. Biomaterials 33, 8062–8074, doi:10.1016/j.biomaterials.2012.07.042 (2012). [PubMed: 22884813]
25. Matthews JA, Wnek GE, Simpson DG & Bowlin GL Electrospinning of collagen nanofibers. Biomacromolecules 3, 232–238, doi:10.1021/bm015533u (2002). [PubMed: 11888306]
26. Yoshimoto H, Shin YM, Terai H & Vacanti JP A biodegradable nanofiber scaffold by electrospinning and its potential for bone tissue engineering. Biomaterials 24, 2077–2082, doi:10.1016/S0142-9612(02)00635-X (2003). [PubMed: 12628828]
27. Xu C, Inai R, Kotaki M & Ramakrishna S Electrospun nanofiber fabrication as synthetic extracellular matrix and its potential for vascular tissue engineering. Tissue Eng 10, 1160–1168, doi:10.1089/1076327041887736 (2004). [PubMed: 15363172]
28. Kurpinski KT, Stephenson JT, Janairo RR, Lee H & Li S The effect of fiber alignment and heparin coating on cell infiltration into nanofibrous PLLA scaffolds. Biomaterials 31, 3536–3542, doi:10.1016/j.biomaterials.2010.01.062 (2010). [PubMed: 20122725]
29. Wang D et al. Proteomic profiling of bone marrow mesenchymal stem cells upon transforming growth factor beta1 stimulation. J Biol Chem 279, 43725–43734, doi:10.1074/jbc.M407368200 (2004). [PubMed: 15302865]
30. Li X et al. Uniaxial mechanical strain modulates the differentiation of neural crest stem cells into smooth muscle lineage on micropatterned surfaces. PLoS One 6, e26029, doi:10.1371/journal.pone.0026029 (2011). [PubMed: 22016804]
31. Pelham RJ Jr. & Wang Y Cell locomotion and focal adhesions are regulated by substrate flexibility. Proc Natl Acad Sci U S A 94, 13661–13665, doi:10.1073/pnas.94.25.13661 (1997). [PubMed: 9391082]

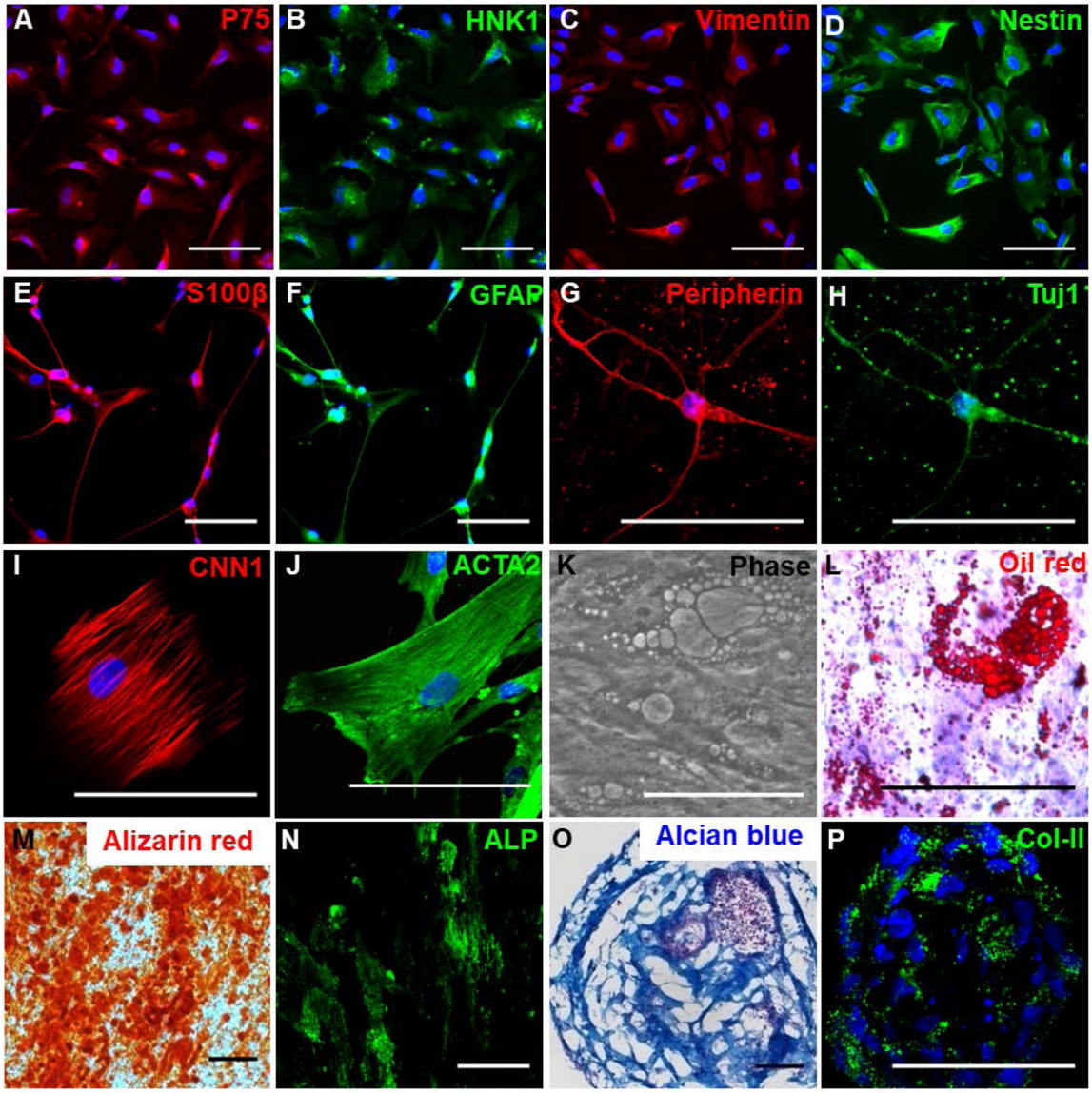

Figure 1.

Characterization of undifferentiated iPSC-NCSCs (A-D) and *in vitro* differentiation potential of iPSC-NCSCs into neural lineages (E-H) and mesenchymal lineages (I-P). (A-D) Immunostaining for NCSC markers P75 (A), HNK1 (B), Vimentin (C) and Nestin (D). (E-F) Immunostaining for Schwann cell markers S100β (E) and GFAP (F). (G-H) Immunostaining for peripheral neuron markers peripherin (G) and Tuj1 (H). (I-J) Immunostaining for SMC lineage markers calponin-1 (CNN1) (I) and smooth muscle α-actin (ACTA2) (J). (K-L) Adipogenic differentiation shown by phase contrast imaging (K) and Oil red staining (L). (M-N) Osteogenic differentiation shown by Alizarin red staining for calcified matrix (M) and immunostaining of alkaline phosphatase (ALP) (N). (O-P) Chondrogenic differentiation shown by Alcian blue staining for glycosaminoglycans (O) and immunofluorescent staining of Collagen-II (P). In all immunofluorescence images, nuclei were stained by DAPI in blue. Scale bar=100 μm.

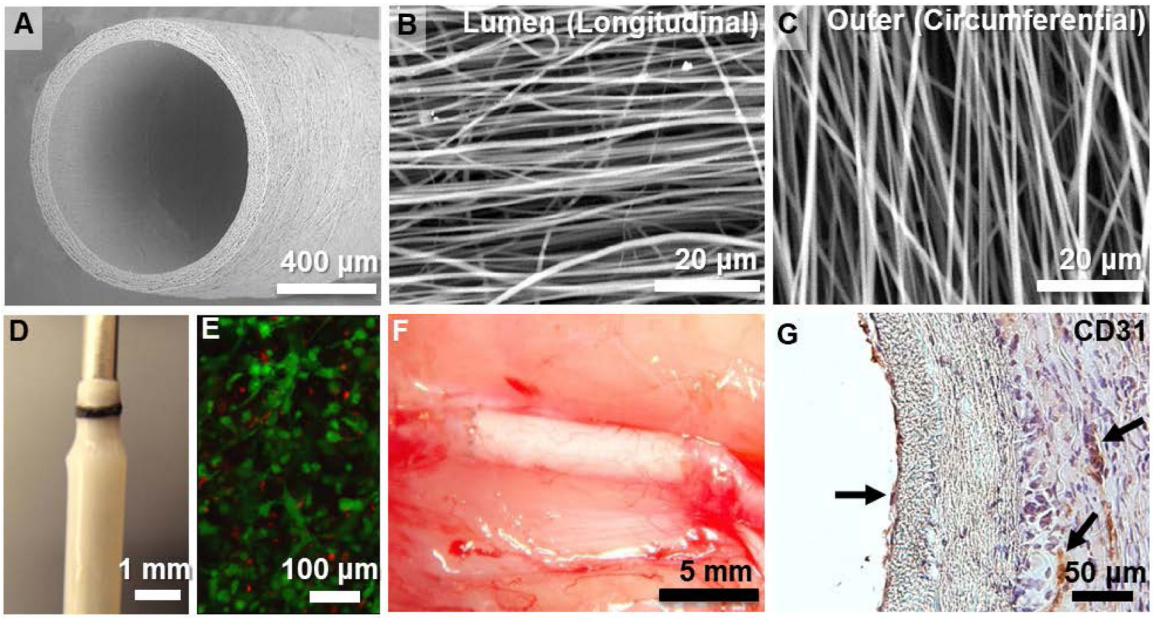

Figure 2.

Cell-seeded nanofibrous vascular scaffold and implantation. (A) SEM image of a nanofibrous vascular scaffold (1-mm inner diameter, 100-μm thickness). Scale bar=400 μm. (B-C) SEM images of a nanofibrous vascular scaffold showing longitudinally aligned fibers in luminal layer (B) and circumferentially aligned fibers in outer layer (C). Scale bar=20 μm. (D) Matrigel layer with NCSCs wrapped around the nanofibrous vascular graft after 1-day culture. Scale bar=1 mm. (E) Live/dead assay after cellular vascular graft fabrication. Green=calcein+ (live) cells. Red=ethidium bromide+ (dead) cells. Scale bar=100 μm. (F) Nanofibrous vascular graft with NCSCs after 3 months of implantation. Scale bar=5 mm. (G) H&E and CD31 staining of a cross section of nanofibrous vascular graft with NCSCs after 3 months of implantation. Arrows show positive staining of CD31. Scale bar=50 μm.

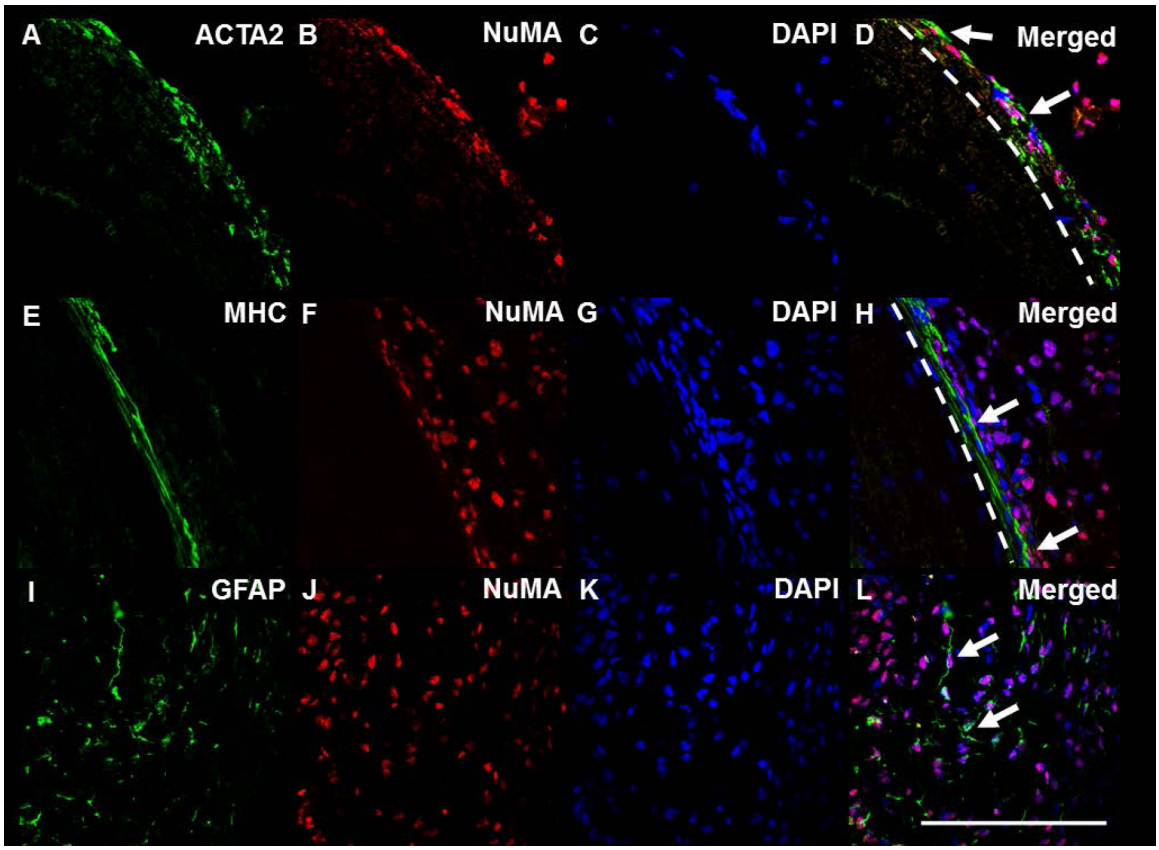

Figure 3.

In vivo differentiation of NCSCs. Vascular grafts with NCSCs embedded in matrigel were implanted for 3 months. SMC markers ACTA2 (A) and MHC (E) or neural marker GFAP (I) were co-stained with human nuclei antigen NuMA (B, F, J). Nuclei were stained by DAPI in blue (C, G, K). The merged fluorescent staining is shown in D, H and L. White dashed lines show the boundary of the fibrous capsule layer. Panels I – L show the area far away from the graft. Arrows show positive staining of ACTA2, MHC or GFAP. Scale bar=100 μm.

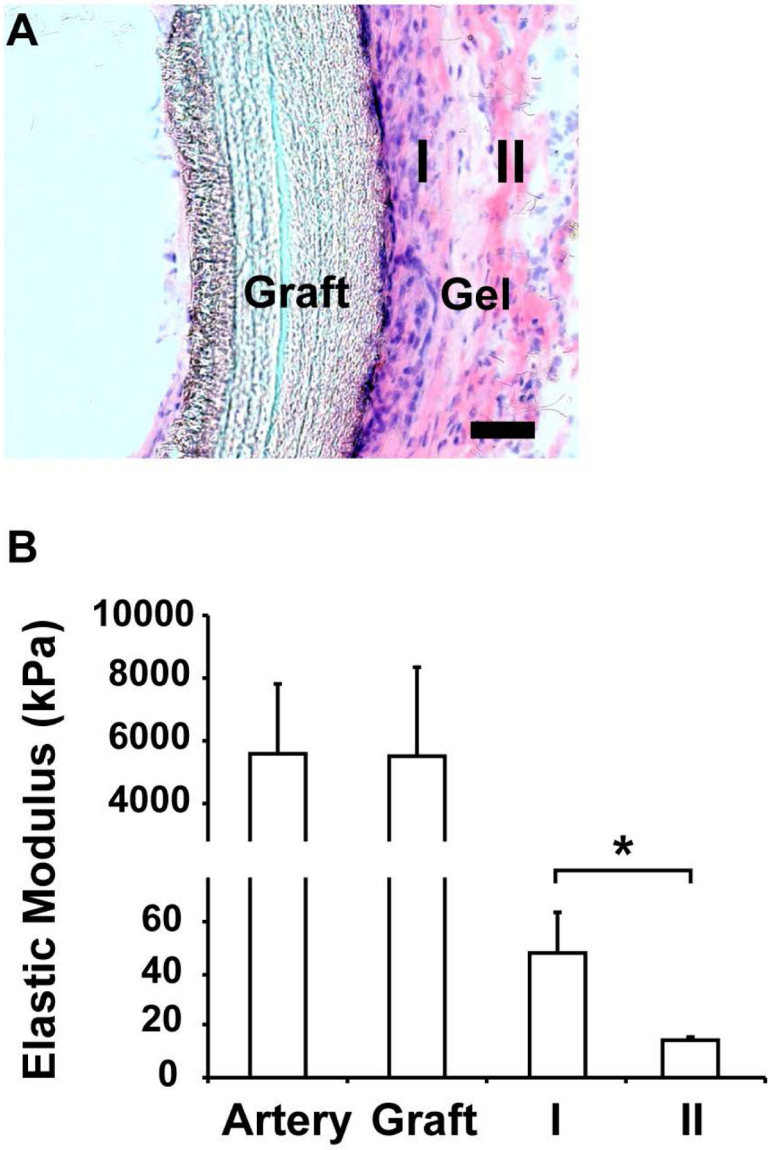

Figure 4.

Elastic modulus of the vascular graft after 3-month implantation. (A) H&E staining of vascular graft. Scale bar=50 μm. (B) AFM measurement of elastic modulus of the nanofibrous vascular graft (n=3) and surrounding matrix with a distance from graft. I:<50 μm from the boundary of polymer graft. II: >100 μm from the boundary of polymer graft). * indicates significant difference ($P<0.05$).

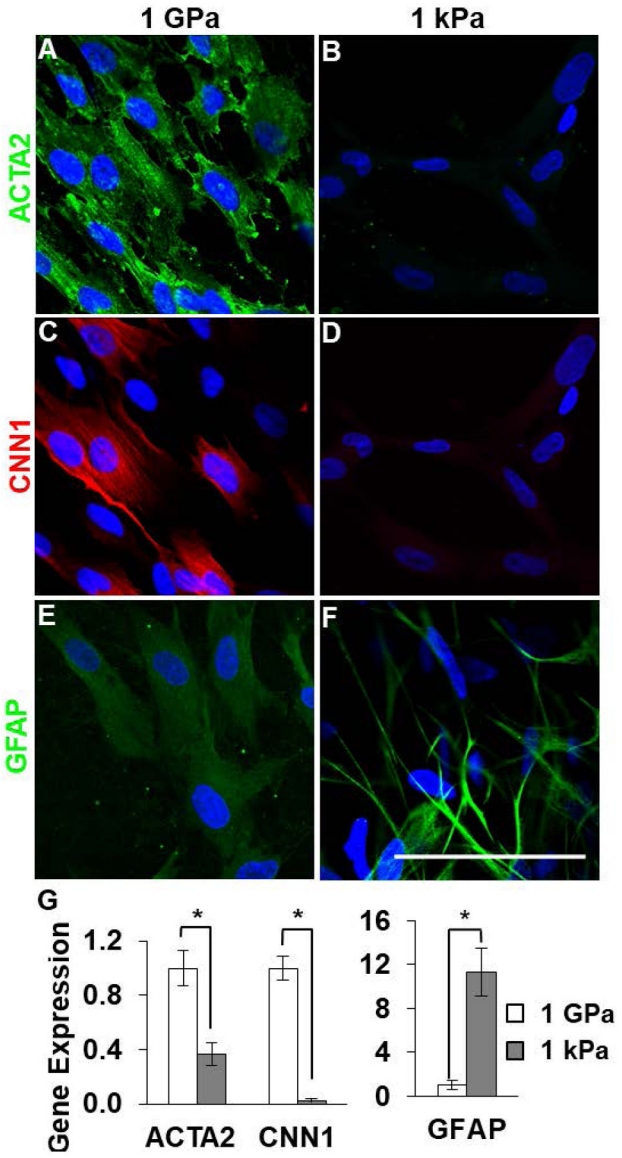

Figure 5.

Effects of stiff and soft surfaces on NCSC differentiation. NCSCs were cultured on matrigel-coated stiff substrates (1 GPa) or matrigel (1 kPa) for 1 week (for immunostaining) or for 3 days (for qPCR). (A-D) Immunostaining for SMC lineage markers ACTA2 (A-B) and CNN1 (C-D). (E-F) Immunostaining for glial cell markers GFAP. Nuclei were stained by DAPI in blue. Scale bar=100 μm. (G) Gene expression ACTA2, CNN1 and GFAP was analyzed by qPCR analysis. * indicates significant difference ($P<0.05$).

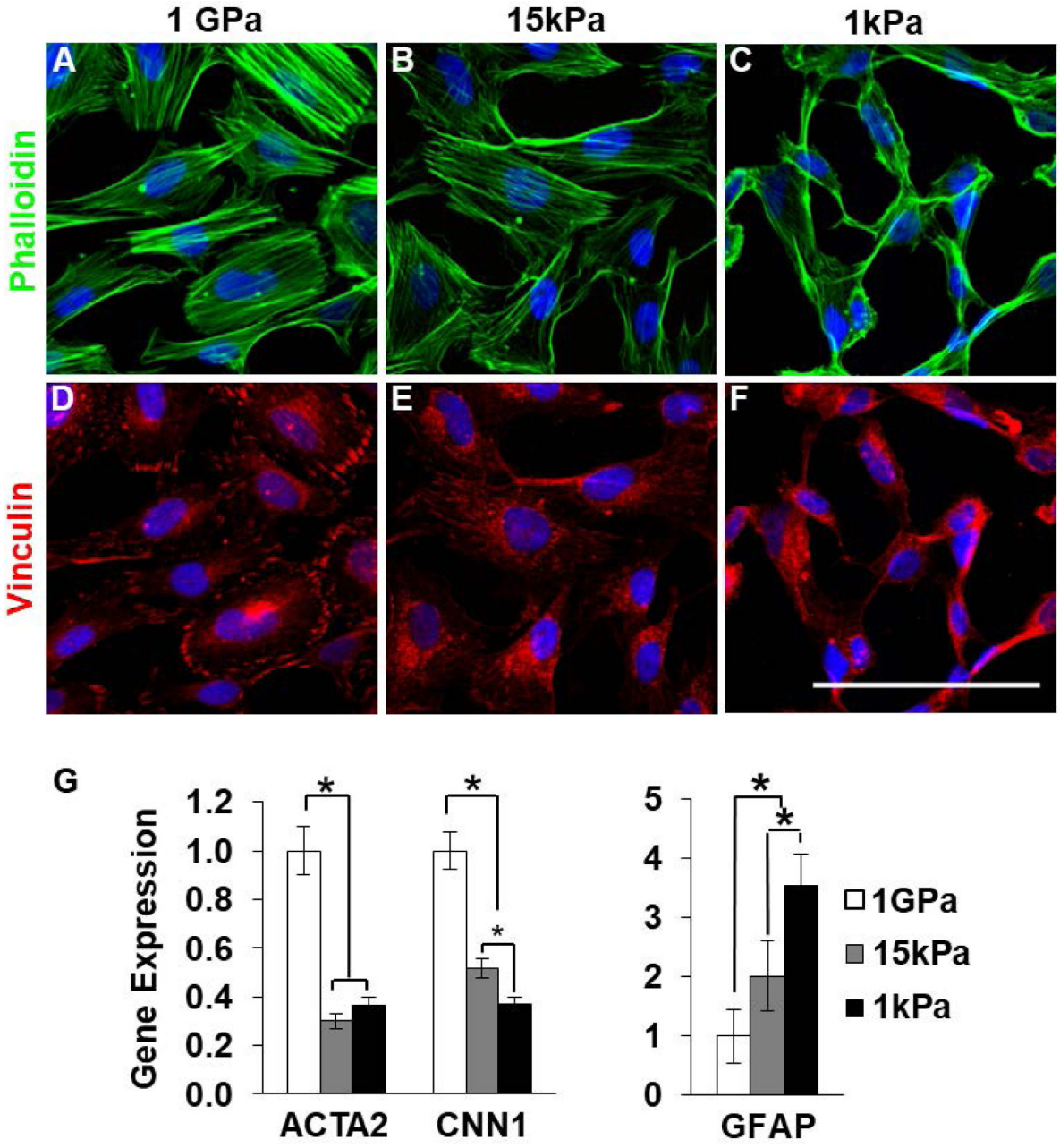

Figure 6.

Effects of substrate stiffness on NCSC morphology. (A-C) Phalloidin staining of F-actin and (D-F) Vinculin staining of cell adhesion after 1-day culture of NCSCs on the stiff substrates (1 GPa) or PA gels using 6% acrylamide and different bis-acrylamide concentrations (Stiffness=15 kPa, 1 kPa). In all immunofluorescence images, nuclei were stained by DAPI in blue. Scale bar=100 μm. (G) Effects of substrate stiffness on NCSC differentiation. NCSCs were cultured on collagen-coated stiff substrates (1 GPa) or PA gels (Stiffness=15 kPa, 1 kPa) for 3 days. Gene expression of ACTA2, CNN1 and GFAP was analyzed by qPCR analysis. * indicates significant difference ($P<0.05$).